THE AMERICAN SOCIETY OF MECHANICAL ENGINEERS
Three Park Avenue, New York, N.Y. 10016-5990

99-GT-354

STUDY OF THE FILTRATION PROCESS THROUGH A CERAMIC CANDLE FILTER

M. Al-Hajeri, A. Aroussi, S. J. Pickering
University of Nottingham, Mechanical Engineering Dept., Nottingham NG7 2RD

ABSTRACT

Ceramic candle filters have been developed for cleaning high-temperature high-pressure (HTHP) gas streams. They meet environmental and economical considerations in Combined cycle power plant, where gas turbine blades can be protected from the erosion that occurs due to using HTHP exhaust from the fluidized bed. Ceramic candle filters are the most promising hot gas filtration technology, which has demonstrated high collection efficiencies et high-temperature high-pressure conditions.

This paper reports a computational fluid dynamics (CFD) investigation of a candle filter. Constant filtration velocity boundary models have been used to investigate the filter in cross flow conditions using the CFD code FLUENT. Different approach (inlet) velocity to filter face velocity ratios and different face velocities (ranging from 2 to 5 cm/s) are used in the CFD calculation. Particles in the diameter range 1 to 100 microns are tracked through the domain. The radius of convergence (or the critical trajectory) is compared and plotted as a function of many parameters. The deposition process and the factors that affect the build up of the filter cake have also been studied.

INTRODUCTION

The conditions of a high temperature high pressure (HTHP) gas between the pressurized fluidized bed combustion (PFBC) and the gas turbine in the combined cycle are of the order of 10-15 bar and 850 °C. This is beyond the range of the conventional methods for gas cleaning except cyclones which have high pressure drop in the range of 50-150 kPa. Two stages of cyclone cleaning are required to meet the dust emission standards and to protect the reggedized gas turbine blades from damage. Rigid ceramic filters are better solution for gas turbine application, with lower pressure drop of less than 25 kPa. The ceramic candle filter is the most promising technology for HTHP filtration due to its ability to resist high temperature conditions and having high collection efficiency.

Ceramic candle filter elements are shaped cylindrically with each element having one of its ends closed. The dimensions are 60 mm outer diameter, 30 mm inner diameter and 50 cm the length. The elements consist of an inner support made from silicon carbide granules with a thin outer layer composed of fine alumina fibers and silicon carbide grains. These elements are combined in a filter vessel where the dirty gas is outside the elements. The cleaned gas is passed to the inside of the candle. The elements are cleaned by back-pulsing to remove the filter cake. The aim of this work is to carry out a parametric study for ceramic candle filter in various arrangements

PREVIOUS RELEVANT WORK

Various HTHP filtration technologies have been investigated by researcher since the mid 1980s. Chang et al (1986), Foote (1986) and Lippert et al (1986) studied ceramic fabric filters or baghouses. Whilst Foote (1986), McEvoy (1986) and Rinard et al (1986) studied electrostatic precipitation. Also, cross-flow filtration was studied by Lippert et al (1986), along side pulsating pressure filtration by kerr (1985) and granular bed filtration and cyclones by Wenglarz et al (1982).

In the case of a ceramic candle filter further investigations were carried out by Drencker et al (1987), Eggerstedt et al (1986), Stringer et al (1992), Higashi (1992) and Aroussi et al (1996). At Aachen University (EPRI (1992)vol 2), an array of six candle filter elements was mounted downstream of a combuster in experimental study. Whilst an array of 130 candle filter elements were investigated at Grimethorpe (EPRI (1992)vol 1). The ceramic candle filters were tested demonstrational at various operating conditions to investigate the back pulse cleaning and cycle time duration. Simmons et al (1998) studied experimentally the flow around the single ceramic candle filter using the particle image velocimetry (PIV) experimental technique.

NOMENCLATURE

d_p- particle diameter.
d_f- filter diameter.
R_f- filter radius
R_{cr}- analytical radius of convergence
D_L- separation of the last impinging trajectory
R_c- radius of convergence.
Re- Reynolds number.
R_d- D_L/d_f Ratio
St- Stokes number.
V - velocity.
V_f- face velocity or filtration velocity.
V_i- upstream approach velocity or inlet velocity.
V_R-Velocity Ratio (V_i/V_f).
μ- viscosity.
ν - kinematics viscosity.
ρ_p- density of particle.
cvcf- constant velocity cross flow

GEOMETRY

The Grimethorpe report (EPRI (1992)vol 1) investigated an array of 130 candle filter elements which are made by Schumacher and assembled in a radial arrangement. These filter elements have an inner diameter of 30 mm and 15 mm wall thickness. In this study, a

Presented at the International Gas Turbine & Aeroengine Congress & Exhibition
Indianapolis, Indiana — June 7–June 10, 1999

single ceramic candle filter is considered and figure 1a shows the two- dimensional physical outline of the model. These dimensions are used in this investigation and figure 1b shows the dimensions of the full computational geometry which is used for the present CFD calculations.

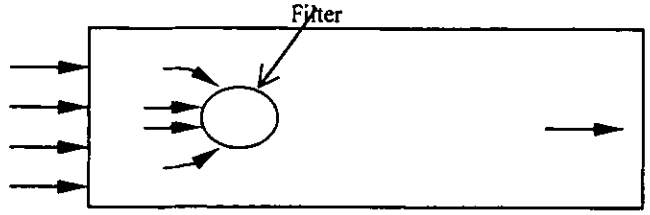

Figure 1a. Single ceramic candle filter in cross flow.

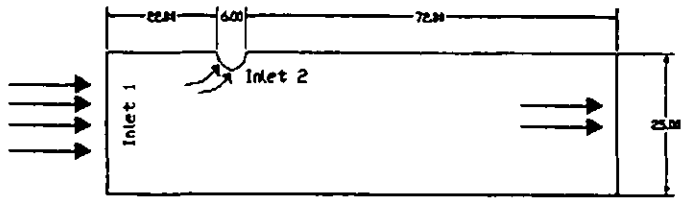

Figure 1b. Computational geometry of single candle filter in centimeter.

The computational domain models are a two-dimensional horizontal slice of a single filter through an array of the candle filters, and only half of the geometry is modeled to save computational time and space. Body fitted co-ordinate grid of 160x80x1 (12800) computational cells constructed in FLUENT's mesh generation preBFC.

Boundary Conditions

This model has two inlets. The main inlet in the problem is referred to as inlet 1. This is an external boundary pre-defined inlet velocity (V_i) set for each case according to the face filtration velocity (V_f) and velocity ratios. Here, the inlet velocity is approach velocity of the flow. Due to CFD's inability to model porous outlets that are not attached to the physical boundaries of the problem, an alternative method to define the outlet as a set inlet boundary at the face of the filter with appropriately defined constant velocity is employed. That is the simplest boundary condition to use and is appropriate because of high-pressure drop across the filter element relatively low gas velocities. This will also solve the problem of not being able to define more outlets than inlets.

The second inlet in the geometry is that at the face of the filter, and it is modeled as a half cylinder, and it is clearly shown in figure 1. Assuming a constant pressure drop across the filter element, a constant face velocity at the inlet 2 must prevail. However, constant u-velocity or v-velocity boundary condition cannot be achieved. Instead, polynomial curve fitted function boundary condition can successively apply and will give a constant face velocity (V_f) at any radii around the filter element.

A third degree polynomial curve fitted function is used in cross flow constant velocity cases (CVCF) to specify x and y velocity components of various locations, around the circumference of the filter. A variety of V_i values are obtained, by assuming various velocity ratios between velocities V_i and V_f and using various face velocities. These values are then set as boundary conditions at inlet 1. In total four different face velocities where used along with six different face velocity ratios. This gives 24 different cases listed in table 1 and used for this study. The face velocities are found at Grimethorpe investigation (EPRI (1992)vol 1).

Grid Independence

It is important to check grid dependency. To achieve grid independence, a finer grid is modeled but with the same geometry, boundary conditions, turbulence models and physical parameters. For the cases studied in this investigation three refinements considered. These grids had 3321(coarse), 12800(fine), and 50244(very fine) cells.

Case no.	V_f(cm/s)	V_i/ V_f	V_i(cm/s)
1	2	0.8	1.6
2	2	1	2
3	2	1.2	2.4
4	2	1.6	3.2
5	2	2	4
6	2	5	10
7	3	0.8	2.4
8	3	1	3
9	3	1.2	3.6
10	3	1.6	4.8
11	3	2	6
12	3	5	15
13	4	0.8	3.2
14	4	1	4
15	4	1.2	4.8
16	4	1.6	6.4
17	4	2	8
18	4	5	20
19	5	0.8	4
20	5	1	5
21	5	1.2	6
22	5	1.6	8
23	5	2	10
24	5	5	25

Table 1 Velocity boundary conditions and velocity ratios used in CVCF cases (V_f is face velocity, V_i is approach velocity)

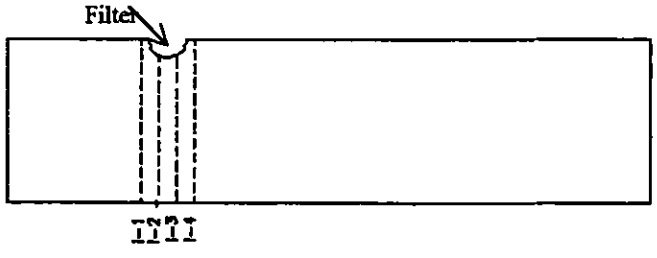

Figure 2. Location of the velocity profiles used for grid independence

The criteria of comparison used to confirm grid independence is velocity magnitude profiles for four different I-planes and it called here I-node. Figure 2 shows the location of each node in the geometry. I-nodes 1, 2, 3 and 4 are at x-distance from inlet 1 of

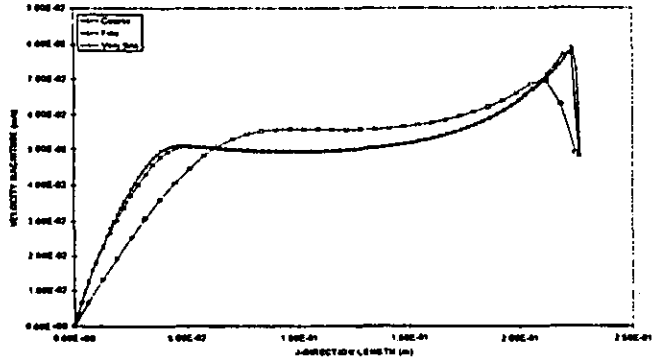

Figure 3a. Velocity magnitude profile for different grids (coarse, fine, very fine) for location I-1.

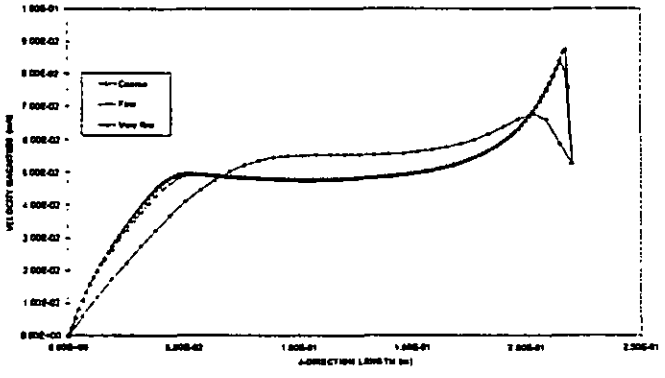

Figure 3b. Velocity magnitude profile for different grids (coarse, fine, very fine) for location I-2.

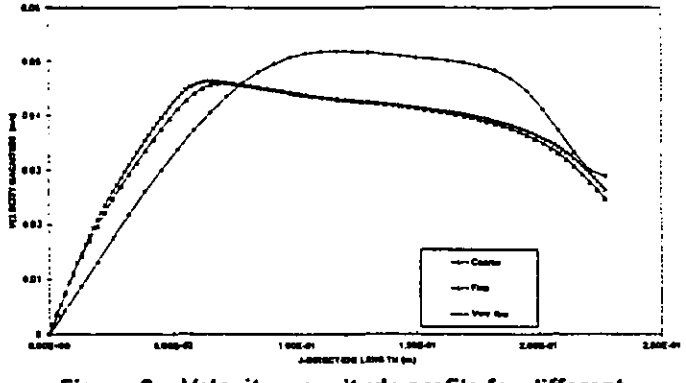

Figure 3c. Velocity magnitude profile for different grids (coarse, fine, very fine) for location I-4.

21, 23.5, 26.5 and 29 cm respectively. Figure 3 shows that the profiles obtained with the fine and very fine grids are identical. However, there are big differences between these two profiles and those obtained in the coarse grid. Fine grid is used through out this investigation.

Selection of the Mathematical Model

For any fluid problem, it is very important to check initially whether the flow is laminar or turbulent and if the flow is turbulent, what type of turbulence model is suitable for the flow. For the inlet velocity range 0.016 to 0.1 m/s used in this investigation, the maximum and the minimum Reynolds numbers for this range are 61.4 and 383.8 respectively .The diameter used in this calculation is the filter element diameter and air assumed to be the working fluid.

However, Simmons et al [1998] reported that experimental velocity profiles obtained using the particle image velocimetry (PIV) technique matched closely results obtained from commercial CFD package, FLOW3D or CFX. Hence, laminar assumption has been used all over the Simmons study.

It has been decided to carry out a comparative study to check upon the most suitable scheme. Three cases are modelled with different mathematical turbulence models, laminar, k-ε turbulence model and RNG k-ε based turbulence model (renormalization group). Grid, physical parameters and boundary conditions are the same in these three cases and the only change is in the type of mathematical model.

RNG k-ε model can be applied for low Reynolds-number situations. For instant, the RNG model can be used when both a turbulent region and a laminar region exist in a domain (FLUENT 1996). Results obtained from this comparative study demonstrated that the RNG k-ε model and the laminar calculations agreed very well whilst the standard k-ε model different substantially from both. This coupled with the findings of Simmons et al (1998) make the use of the laminar solution method more representative and computationally very economical. This is particularly true, since the effects of the filter act as a boundary layer bleeding mechanism and justify the laminar flow assumption.

Results of the Parametric Study

The aim of this work is to carry out a parametric study for ceramic candle filter in various arrangements. The flow around the filters may be categorized as cross flow, parallel flow or turning flow. The flow at the outside of the filter array is usually cross flow but in the middle becomes parallel flow while at the bottom of the array the flow is turning flow (EPRI (1992)vol 1). The face velocity into each filter is the same irrespective of the position in the array, as the pressure difference across each element is large compared to the dynamics pressure of the flow approaching and within the filter array.

Since the filters are quite long (50 cm) relative to their diameter (6 cm), this arrangement becomes very similar to that for flow around tube banks. However, an important difference here is the existence of normal velocity component to the filter element due to the filtration effect. This is a point that will legitimize a two-dimensional treatment, where cross flow is concerned, is realistic. A further simplification to the problem is through the use of a symmetry line through the centerline of a single filter element as shown in figure 1c.

Particle trajectories around single filter were investigated for different size, face velocities and inlet velocities. Face velocities will vary and values of 2, 3, 4 and 5 cm/s which are found at Grimthorpe (EPRI (1992)vol 1), are used. Inlet velocities vary according to the velocity ratio V_i/V_f, and V_i/V_f ratios range of 0.8, 1, 1.2, 1.6, 2 and 5 are used. Table 1 shows the 24 boundary condition which are used here in this study.

Radius of Convergence

One of the main objectives of this work is to carry out a parametric study of the flow around the ceramic candle filter. A radius of convergence (R_c) as defined by Aroussi et al (1996) is a useful comparison criteria. It is defined as the distance from the filter centerline, at the main inlet, to the position of injection of the last

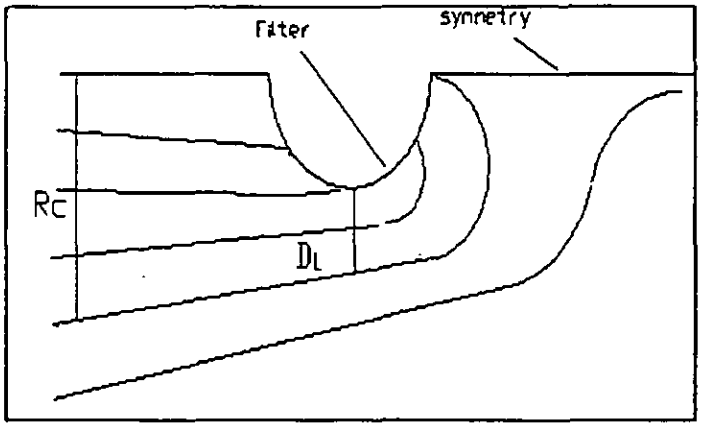

Figure 4. Definition of R_c and D_L

particle which will impinge on the filter. Figure 4 shows the definition of the radius of convergence which is also called, the critical trajectory. The radius of convergence depends upon the inlet velocity, the particle size and the face velocity.

The calculation is a time consuming repetitive process where particles are injected at the inlet into the domain. This is repeated at various levels until a particle turning around the filter impinges on it at the point closest to the symmetry line behind the element. Spherically shaped particles having diameter of 1, 50 and 100 microns were injected with an assumed density of 1000 kg/m^3. Although, particle diameters between 1 to 50 microns are the main focus here, the results show that no change in the trajectory occurred for particles in the range 1 to 50 microns in cross flow investigation. However, radius of convergence varies if the particle has diameter of 100 microns and larger.

Figure 5 shows the relation between the radius of convergence (R_c) and the inverse of the inlet velocity ($1/V_i$) for the face velocity of 3 cm/s. The curves are straight line and show R_c for the three size particles 1, 50 and 100 μm. Those curves are identical but there are slight differences in the case of the high inlet velocity with particle size of 100 μm (as stated earlier).

For the case of the face velocity of 5 cm/s, figure 6 shows the relationship between the radius of convergence and $1/V_i$. The graphs are straight lines and, as in the previous figure. at high inlet velocity, the radius of convergence (R_c) for particle size of 100 μm diverges slightly in value. Overall, the three graph curves for 1, 50 and 100 μm have identical values for the radius of convergence. For four other velocities 2, 3 and 4 m/s, the curves have the same trends, however they have different values for the radius of convergence at different inlet velocities. So as the inlet velocity is increased, whilst the face velocity is kept constant, the radius of convergence is decreased. In conclusion, the V_i/V_f ratio is the main factor affecting the radius of convergence in the cross flow regime. The graph curves show that as the V_i/V_f ratio (V_R) decreases the radius of convergence increases.

Stokes Number

Non dimensional analysis is a very useful comparison tool in the present problem. The Stokes number is appropriate for fluid-solid flow, and using Buckingham π- Theorem, Stokes number is defined by using the approach velocity as,

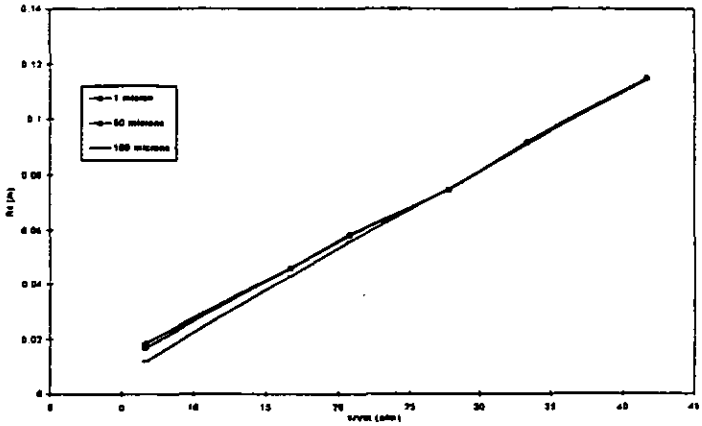

Figure 5. Variation of R_c with V_i for particle diameter of 1, 50 and 100 microns. (V_f=3 cm/s)

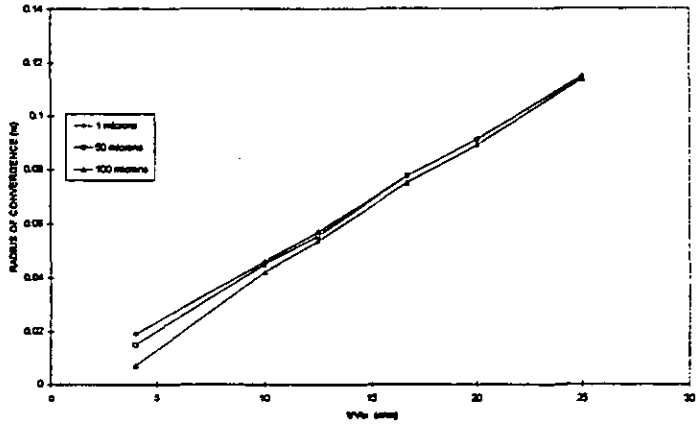

Figure 6. Variation of R_c with V_i for particle diameter of 1, 50 and 100 microns. (V_f=5 cm/s)

$$St = \frac{\rho_p d_p^2 V_i}{18 \mu d_f} \qquad (1)$$

Stokes number results are plotted here in two graphs with respect to non-dimensional radii of convergence. The radius of convergence (Rc) is divided by the filter diameter to obtain a non-dimensional form of R_c. Figure 7 shows the relationship between the radius of convergence to filter diameter with Stokes number for particle size 50 μm. The horizontal straight lines for each V_i/V_f ratio indicate that the radius of convergence does not change with Stokes number regardless of whether the face velocity or the inlet velocity is used for any particle having a diameter less than 100 microns. If particle diameter is increased and V_i/V_f ratio is kept constant, the radius of convergence decreases. Stokes number values range between 1 to 2.5 in the case size of 1 μm particles, and between 50 to 125 in case of 50 μm particles.

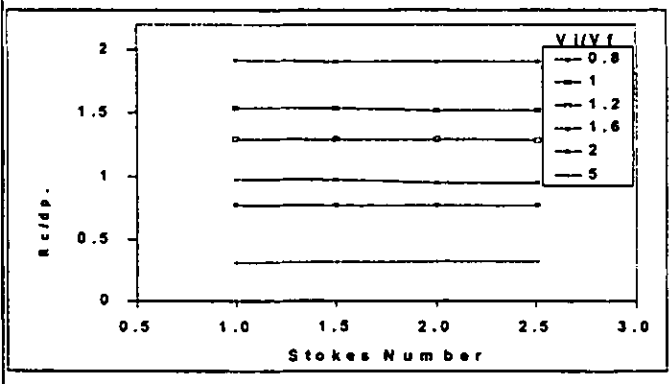

Figure 7. Variation of Stokes number with V_i for particle diameter of 50 microns. (V_f=5 cm/s)

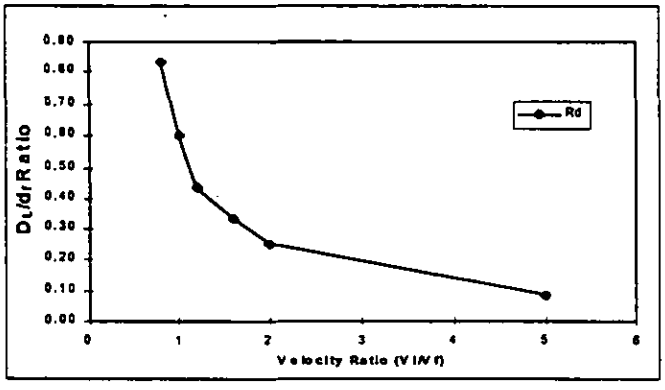

Figure 8. Variation of DL/d_f with V_i/V_f. (V_f=2 cm/s)

Separation of the last impinging trajectory (D_L)

One of the important factors in designing ceramic candle filters or in the investigations of multiple filters is the spacing between any two-filter elements. Determining the spacing between the filters pre-requisites the knowledge of the radius of convergence and the V_i/V_f ratio which the filter will operate at. A new parameter (D_L) is introduced in this study which is the distance between the particle path of the furthest impinging trajectory and the surface of the filter nearest to it as shown in figure 4. This distance is measured perpendicular to the centerline in the present solution domain. This parameter is then used to define an important non-dimensional ratio R_d which is the ratio of the separation of the last impinging trajectory (D_L) to the filter diameter (D_L/d_f). D_L values are calculated based on particle trajectories of particle sizes of 1, 50 and 100 μm.

Figure 8 exhibits a plot of the D_L/d_f ratio against V_i/V_f. This is also shown in table 2 where D_L/d_f decreases with increase in V_i/V_f. However, as the inlet (approach) velocity increases whilst the face velocity is kept constant, the filter suction (and D_L consequently) will both decrease. Filter elements should, hence, be designed faraway from each other in the case of lower V_i/V_f ratios and close to each other in the case of higher V_i/V_f ratios. For rows of filters nearer to the inlet in an array, the filter elements should be spread out further to allow flow to pass in between to the next raw. Also, trends of change in D_L/d_f ratio and D_L are identical for all V_i/V_f ratio cases regardless of the change in face and inlet velocity.

V_i/V_f	$R_d=(D_L/d_f)$	R_C (cm)	D_L (cm)
0.8	0.837	0.115	0.050
1	0.598	0.092	0.036
1.2	0.434	0.0745	0.026
1.6	0.325	0.0585	0.020
2	0.249	0.046	0.015
5	0.079	0.0184	0.005

Table 2 R_d (D_L/d_f ratio) and particle path distance. V_i = 2 cm/s

Particle Deposition Distribution

Particle deposition is needed to understand the build-up of filter cake over the filter surfaces to design efficient cleaning mechanisms. If the particles following the fluid path deposit

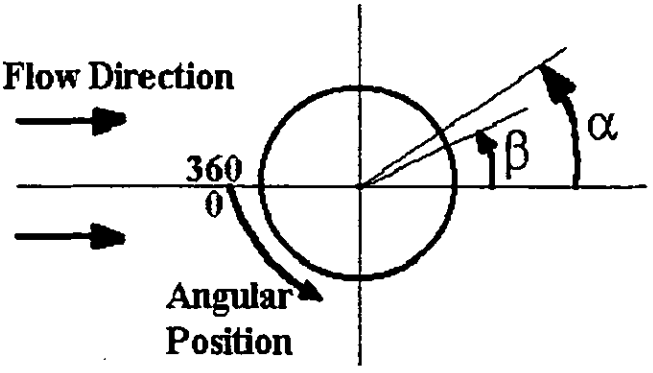

Figure 9. Uniform (α) and ununiform deposition (β) on the filter

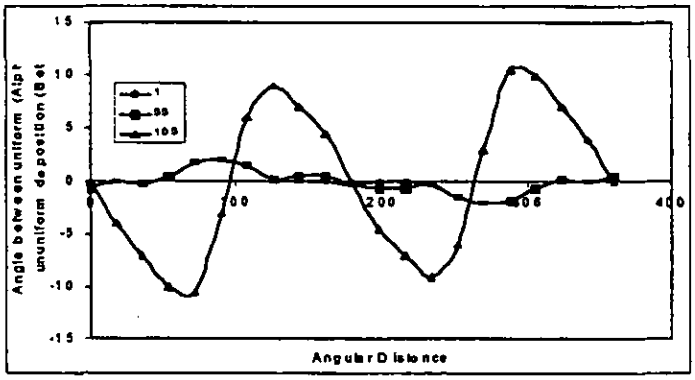

Figure 10. Particle distribution for 50 microns Particles (V_f=5 cm/s)

uniformly over the filter surface, the angle between the downstream horizontal centerline of the filter and the deposition point in the element is alpha (α) as shown in figure 9. However, if the flow is non-uniform, such that the particle path splits from its related fluid stream and deposits on the filter at different point, the new shifted

particles deposition angle is called beta (β). Where (α-β) becomes the angular shift (difference) in the deposition.

Figure 10 shows the angular difference in the deposition (α-β) as opposed to the angular position around the filter from the fluid stagnation point upstream the filter. The graph also shows the effects of particle sizes of 1, 50 and 100μm at $V_i/V_{f\,ratio}$ of 2 and face velocity of 5 cm/s. For particle sizes of 1 to just less than 100μm, the deposition is uniform and following the fluid stream. However, at particle size of 100μm and larger, a non-uniform particle distribution pattern begins to appear. This result is comforting since in practice particles reach the ceramic candle filter are usually less than 50μm in diameter, hence, a uniform particle distribution would be expected.

Analytical Solution for the of Radius of Convergence

Analytical estimations for the radius of convergence for a fluid particle can be performed using a mass conservation for cross flow,

$$\pi R_f V_f = R_{cr} V_i \qquad (2)$$

$$R_{cr} = \frac{2\pi R_f V_f}{V_i} \qquad (3)$$

Inlet velocities can be obtained by applying equation 3 for face velocities of 2, 3, 4 and 5 cm/s and V_i/V_f ratios of 0.8, 1, 1.2, 1.6, 2 and 5. A number of these conditions are used to create a variety of operating conditions. This gives 24 cases in total, where several analytical radii of convergence are obtained.

Analytical results obtained from equation 3 are plotted and compared with results obtained from CFD for the same parameters; namely the inlet and the face velocities. CFD results for the radius of convergence (V_i = 2 cm/s) are given in table 2 whilst figure 11 shows the analytical and CFD results for R_c at an inlet velocity of 2 cm/s and V_i/V_f velocity ratios of 0.8, 1, 1.2, 1.6, 2 and 5. These results show identical trends and values for the radius of convergence in both, CFD and analytical studies. However, they are slightly differences at V_i/V_f ratio of 0.8. For example, in the case of a face velocity of 3 cm/s and V_i/V_f ratio of 0.8, the difference is 2 % which is very small and may be ignored.

Conclusions

A computational investigation has been carried out into the flow around a single ceramic candle filter element in cross flow. The radius of convergence (R_c), the separation of the last impinging trajectory (D_L) and the velocity fields are used to explain the particles behavior and the filter cake distribution.

Three particle sizes of 1, 50 and 100 microns are tracked through the domain to determine Rc and D_L for several face velocities as well as several (inlet/ face) velocity ratios (V_i/V_F). It is found that the radius of convergence and the separation of the last impinging trajectory (D_L) decrease with the increase of V_i/V_f ratio and the reduction in R_c as the particle size increases. Also it is found that for any Stokes number and particle diameter smaller than 100 microns, Rc is constant. Filter cake distributions around the filter element surface are uniform for particle sizes below 50 microns. Thus, that

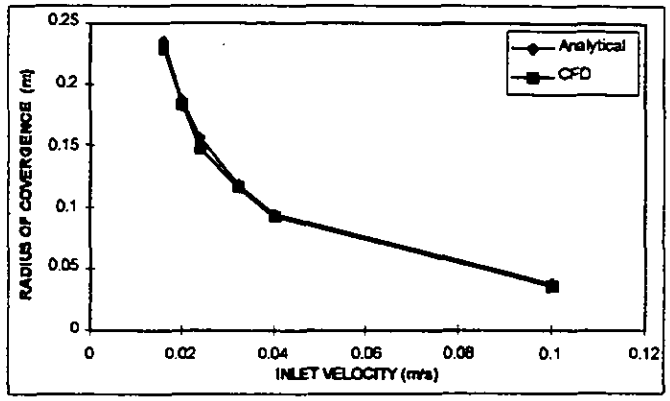

Figure 11. Radius of convergence for analytical and CFD (V_f=2 cm/s)

can delay the cleaning periods and increase the filtration time. Results obtained here are essential for designing the cleaning mechanism after the elements being blocked.

REFERENCES

Aroussi, A., Simmons, K. and Pickering, S. J., 1996, "Removal of particulate material by ceramic candle filter, " IMechE S447/014/96, pp. 193-204.

Chang, R., Sawyer, J., Lips, H., Bedick, R. and Dellafield, R., 1986, "The testing and evaluation of ceramic fabrics, "*6th sympasium an the transfer and utilization af particulate cantrol, New Orleans*, vol. 1, paper 11.

Drencker, S.G., Stringer, J.S., and Tassicker, O. J., 1987, "Pilot scale development of ceramic filters for PFBC power plants, "Proceedings of the 9th international conference on FBC. Vol 2, pp. 1008-1012.

Eggerstedt P., and Zievers, J. F., 1986, "Hot gas clean-up by means of porous ceramic filter elements, " 6th Symposium on the transfer and utilization of particulate control, New Orleans, Vol. 1, paper 12.

EPRI, 1992, High-temperature gas filtration. Vol 2: Operating performance of a pilot-scale filter, EPRI Rept. GS-6489 vol. 2, October.

EPRI, 1992, Grimethorpe high-pressure/high temperature gas filter experimental program, Vol. 1: design, commissioning and modification of a large hot-gas filter on the grimethorpe PFBC. EPRI Rept. TR-100-499 vol. 1, September.

FLUENT, 1996, " FLUENT user's guide," FLUENT Incorporated.

Foote, J.P., 1986, "Design of baghouse and electrostatic precipitator for the coal-fired flow facility, " 6th Symposium on the transfer and utilization of particulate control, New Orleans, Vol. 1, paper 14.

Higashi, O, "Development of high temperature, high-pressure filtration technology, " ASME paper 92-G7-370.

Kerr, K., and Probert, D., 1985, "Pulsating pressure filter for fluidized bed combustion gas clean up, " Applied Energy (UK), Vol 20, n. 2.

Lippert, T. E., Ciliberti, D. F., Tassicker, O. J., and Drencher, S. G., 1986, "Test and development of woven ceramic bag and ceramic candle filters for the HTHP application, " Symposium of cleaning at high temperature, Surrey, pp. 215-231.

McEvoy, L. T., Parker, K. R., and Russel-Jones.A, 1986, "The collection of fine particulate in power plant electrostatic precipitators, "6th Symposium on the transfer and utilization of particulate control, New Orleans, Vol. 1, paper 6.

Rinard, G. A., dugg, D.E., Durham, M., and Armstrong, A., 1986, "Advanced energy application II – Results of parametric tests on an electrostatic precipitator operating at high temperature and high pressure conditions, "6th Symposium on the transfer and utilization of particulate control, New Orleans, Vol. 1.

Simmons, K., Aroussi, A., Pickering, S.J. and Clayton, B.R., 1998, "Particulate material deposition on a ceramic by candle filter," ASME Fluids Engineering Division summer meeting.

Stringer, J., Leitch, A.J. and Clark, R.K., 1991, " THE EPRI hot gas filter pilot plant at Grimethorpe: what worked, what broke and where do we go now?, Fluidized Bed Combustion.

Wenglarz, R. A., and Schneider, J., " An assessment of erosion in PFBC power plant turbines, " ASME paper 82-GT-194.

White, F. M., 1991, "Viscous fluid flow, " McGraw-Hill, New York.